

## Identification of the calcium-dependent gating and targeted-drug discovery of calcium-activated chloride channels

Hailong An, Chunli Pang, Shuai Guo, Yafei Chen and Hailin Zhang

### Abstract

Calcium-actuated chloride channels (CaCCs) assume imperative parts in an assortment of physiological cycles. Transmembrane protein 16A (TMEM16A) has been affirmed as the sub-atomic partner of CaCCs which significantly pushes the sub-atomic experiences of CaCCs forward. Be that as it may, the point by point system of Ca<sup>2+</sup> restricting and actuating the channel is as yet dark. To distinguish the calcium restricting site, the creators introduced a computational methodology which consolidated the piece homology displaying with sub-atomic elements reenactment. Our information show that the main intracellular circle fills in as a Ca<sup>2+</sup> restricting site including D439, E444, and E447. The exploratory outcomes demonstrate that a novel buildup, E447, assumes a vital part in Ca<sup>2+</sup> restricting. Contrasted and WT TMEM16A, E447Y produces a 30-overlap expansion in EC<sub>50</sub> of Ca<sup>2+</sup> initiation and prompts a 100-crease expansion in Ca<sup>2+</sup> focuses that is expected to completely enact the channel. It is grounded that TMEM16A is a medication focus in numerous sicknesses, including cystic fibrosis, hypertension, asthma, and different tumors. Along these lines, recognizing strong and explicit modulators of the TMEM16A channel is essential. Here, the creators distinguished two modulators from the conventional Chinese medication, an activator, Ginsenoside Rb1 (GRb1) which can expand the sufficiency and recurrence of withdrawals in a disconnected guinea pig ileum measure in vivo and fill in as a lead compound for the improvement of novel medications for the treatment of illnesses brought about by TMEM16A brokenness, an inhibitor, matrine which can significantly repress the development of lung adenocarcinoma tumors in xenografted mice, and may

work as an enemy of lung adenocarcinoma drug focusing at TMEM16 channels.

### Methods and Results:

The Ca<sup>2+</sup> affectability of Ano1 was assessed from paces of current enactment, and deactivation in extracted fixes quickly exchanged among nothing and high Ca<sup>2+</sup> on the cytoplasmic side. Transformation of glutamates E702 and E705 drastically modified Ca<sup>2+</sup> affectability. E702 and E705 are anticipated to be in an extracellular circle, however antigenic epitopes brought into this circle are not open to extracellular antibodies, proposing this circle is intracellular. Cytoplasmically applied layer impermeant sulfhydryl reagents change the Ca<sup>2+</sup> affectability of Ano1 E702C and E705C true to form if E702 and E705 are intracellular. Subbed cysteine openness mutagenesis of the putative re-participant circle proposes that E702 and E705 are found adjoining the Cl conduction pathway.

### Conclusions

We propose an elective model of Ano1 geography dependent on mutagenesis, epitope openness, and cysteine-examining availability. This information repudiates the famous re-participant circle model by showing that the putative fourth extracellular circle (ECL 4) is intracellular and may contain a Ca<sup>2+</sup> restricting site. These investigations give new viewpoints on guideline of Ano1 by Ca<sup>2+</sup>.

### Introduction

Calcium-initiated chloride channels (CaCCs) assume crucial parts in the cardiovascular framework. In vascular smooth muscle, vasoconstrictor-activated

Hailong An  
Hebei University of Technology, China, E-mail: hailong\_an@hebut.edu.cn

preparation of Ca<sup>2+</sup> from intracellular stores opens CaCCs that serve in a positive input circle to support compression by depolarizing the layer and initiating Ca<sup>2+</sup> deluge through voltage-gated Ca<sup>2+</sup> channels. In entrance vein smooth muscle, Ca<sup>2+</sup> flashes created from ryanodine-touchy stores can enact CaCCs to produce unconstrained transient internal flows, which depolarize and initiate voltage-gated Ca<sup>2+</sup> channels. In heart myocytes of certain species, including hare, pig, canine, and sheep, yet likely not human, CaCC flows have been displayed to assume a part in cardiovascular activity expected repolarization and to take part in arrhythmogenesis. As of late, it has been recommended that the medical advantages (counting decreased danger of cardiovascular sickness) of red wine and green tea might be clarified by the immediate impacts of gallotannins on CaCCs.

Albeit the cardiovascular meaning of CaCCs has for some time been evident, seeing how these channels work has been delayed to create in light of the fact that the atomic personality of CaCCs was not found until 2008, when three research centers recognized Tmem16A, presently known as anoctamin-1 (Ano1), as a fundamental subunit of CaCCs. Ano1 is an individual from a 10-quality superfamily, of which two individuals, Ano1 and Ano2, have been plainly displayed to encode CaCCs that partake in liquid and salt vehicle by epithelia, moderate wave action in the gut, guideline of smooth muscle withdrawal, and control of cell edginess. Ano1 has been displayed to encode CaCCs in vascular smooth muscles.

Seeing how Ano1 channels work requires information on how Ca<sup>2+</sup> makes the channel open. Indeed, even before CaCCs were recognized at the sub-atomic level, it was seen that the biophysical properties of CaCC flows rely upon Ca<sup>2+</sup> fixation. Submicromolar Ca<sup>2+</sup> enacts a current that emphatically apparently corrects and is time-subordinate, though higher focuses initiate a prompt current with no amendment. This distinction is physiologically pertinent on the grounds that it decides, for instance, regardless of whether epithelial CaCCs work in a secretory or absorptive limit or whether

neuronal CaCCs convey outward or internal current. Notwithstanding, it is cryptic how voltage-ward and Ca<sup>2+</sup>-subordinate gating comes about atomically, to a great extent on the grounds that the area of the Ca<sup>2+</sup> restricting locales and the anion-particular pore stay obscure.

Studies on the construction capacity of Ano1 to date have been directed by a geography model of eight transmembrane  $\alpha$ -helices with a re-participant circle between transmembrane helices 5 and 6. This model depends on hydropathy examination and tests performed on Ano7. Be that as it may, the legitimacy of this model for Ano1 has not been tentatively settled. This is particularly basic on the grounds that Ano7 has not yet been demonstrated to be a Cl channel and in light of the fact that the amino corrosive groupings of Ano1 and Ano7 are just 32% indistinguishable. The putative re-contestant circle has been an excellent suspect for the direct pore in Ano1 in light of the fact that the R621E transformation was accounted for to definitely change the anion-to-cation selectivity of the channel. Investigations portrayed brought up issues in our brain about the area of the pore and invigorated us to reconsider the geography of Ano1 and potential Ca<sup>2+</sup> restricting locales. Our changed model moves the recently assigned fourth extracellular circle to an intracellular area and recognizes a potential Ca<sup>2+</sup> restricting site in this space. This model has the appealing component that it's anything but a Ca<sup>2+</sup> restricting site promptly adjoining the pore and gives experiences into Ano1 channel gating.

## Methods

Techniques have recently been depicted and definite Methods are given in the Online Supplement. The mAno1 a,c join variation (Accession: Q8BHY3) was utilized. Transformations were made utilizing polymerase chain response based mutagenesis. The mouse Ano (mAno)- 1 was transfected into HEK293 cells utilizing Fugene-6; (Roche Molecular Biochemicals). Transfected HEK293 cells were fix cinched utilizing ordinary entire cell and extracted back



to front patches. The zero  $\text{Ca}^{2+}$  intracellular arrangement contained 146 mmol/L CsCl, 2 mmol/L  $\text{MgCl}_2$ , 5 mmol/L EGTA, 10 mmol/L HEPES, and 10 mmol/L sucrose, pH 7.3, changed with NMDG. High- $\text{Ca}^{2+}$  pipette arrangement contained 5 mmol/L  $\text{Ca}^{2+}$ -EGTA, rather than EGTA (free  $\text{Ca}^{2+}$  roughly 20  $\mu\text{mol/L}$ ). The 126  $\mu\text{mol/L}$  and 2 mmol/L  $\text{Ca}^{2+}$  were made by adding 0.2 mmol/L and 2 mmol/L  $\text{CaCl}_2$  to high- $\text{Ca}^{2+}$  arrangement. The standard extracellular arrangement contained 140 mmol/L NaCl, 5 mmol/L KCl, 2 mmol/L  $\text{CaCl}_2$ , 1 mmol/L  $\text{MgCl}_2$ , 15 mmol/L glucose, and 10 mmol/L HEPES, pH 7.4, with NaOH. Relative anion penetrability was controlled by estimating the change in zero-current  $E_{\text{rev}}$  subsequent to changing the shower arrangement from 151 mmol/L  $\text{Cl}^-$  to 140 mmol/L substitute anion ( $\text{X}^-$ ) in addition to 11 mmol/L  $\text{Cl}^-$ .

The penetrability (P) proportion was determined by utilizing the Goldman-Hodgkin-Katz condition. Penetrability of  $\text{Na}^+$  or  $\text{Cs}^+$  comparative with  $\text{Cl}^-$  was dictated by estimating changes in zero-current  $E_{\text{rev}}$  when the grouping of extracellular NaCl or CsCl was changed ("weakening potential" technique). The quick use of  $\text{Ca}^{2+}$  to extracted back to front patches was performed utilizing a twofold barreled theta tubing with a tip distance across of roughly 50  $\mu\text{m}$  connected to a piezobimorph on a micromanipulator.

One barrel was loaded up with standard zero  $[\text{Ca}^{2+}]_i$  arrangement, and the other barrel was loaded up with intracellular arrangement containing the demonstrated free  $\text{Ca}^{2+}$ . The time course of arrangement trade across the laminar stream interface was assessed by fluid intersection expected estimations to be 0.5 ms (10% to 90% ascent time) for a 10-crease contrast in ionic strength. The mAno1 with embedded human flu hemagglutinin (HA) epitopes at different positions were utilized to decide the geography by evaluating the availability of the HA epitope to extracellularly applied counter acting agent. Cells were fixed for 15 minutes at room temperature in 1% paraformaldehyde in 0.1 mol/L phosphate cushion (pH 7). Nonpermeabilized cells were

washed in multiple times in impeding cushion. Permeabilized cells were hatched in impeding cushion containing 0.15% to 0.3% Triton-X100. Cells were hatched with against HA counter acting agent weakened 1:750 in obstructing support for 2 hours at room temperature, washed multiple times in hindering cradle, and afterward brooded in goat-antirabbit IgG formed with Dylight-549 (Jackson Immunochemicals).

## Results

### Topology of mAno1

We utilized 14 distinctive web workers utilizing various systems to anticipate mAno1 transmembrane spaces (Online Table I). All calculations reliably distinguished seven portions comparing to transmembrane spaces 1 to 4 and 6 to 8 in Figure 1B (left board). Two calculations neglected to recognize transmembrane space 5 and five calculations distinguished the proposed re-contestant circle as a transmembrane area. Considering this uncertainty, we needed to explain Ano1 geography. We brought HA epitopes into mAno1-EGFP at different positions (570, 614, 672, 700, or 824; Figure 1A), communicated the builds in HEK cells, and afterward assessed the availability of the acquainted epitopes with extracellularly applied antibodies in permeabilized and nonpermeabilized cells by confocal microscopy. We initially performed fix clasp recording to confirm that the presentation of the epitope didn't annihilate channel work.

The entirety of the develops showed flows normal for Ano1 (Figure 1A, right table) and mAno1-EGFP fluorescence at the layer (Figure 1A, left boards), demonstrating that the HA inclusions didn't fundamentally modify the tertiary design of the channel. In nonpermeabilized cells, HA epitopes were available to extracellular enemy of HA immune response just at positions 614 and 824 (Figure 1A, center boards); the wide range of various positions were distant. The unavailability of the epitopes presented at 672 and 700 isn't steady with the geography displayed in Figure 1B (left board) and proposes that the putative extracellular

circle 4 (amino acids 650–706) is arranged intracellularly.

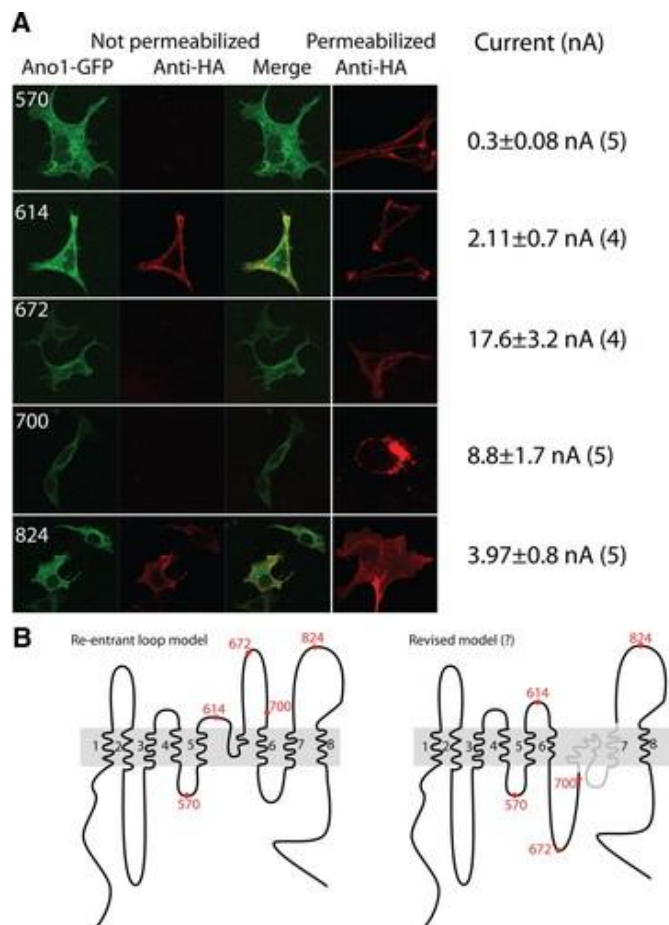


**Figure 1. Immunofluorescent staining of mAno1 containing tandem hemagglutinin (HA) epitopes inserted at various locations.**

**A**, HA tags were inserted into mAno1-EGFP at amino acids 570, 614, 672, 700, and 824. After transient expression, nonpermeabilized intact cells were stained with antibody for HA epitope. Green: Ano1-GFP; red: anti-HA and merged image. Duplicate cover slips were permeabilized before incubation with HA antibody (red: permeabilized, anti-HA). For each construct, images were acquired at the same gain and settings, but settings may differ between constructs that were imaged on different days. Raw images from the Zeiss Zen acquisition software from permeabilized and nonpermeabilized cells were assembled in Adobe Photoshop CS5 and brightness-adjusted and contrast-adjusted for all four panels equally. Anoctamin-1

(Ano1) currents for each construct were recorded with 20  $\mu\text{mol/L}$  Ca. Average peak amplitude at +100 mV and the number of recorded cells are listed. **B**, Topological models of mAno1. The locations of HA tags are indicated with red numbers. **Left**, Re-entrant loop model. **Right**, revised model. The topology of the sequence depicted in gray remains in question.

### E702 and E705 Contribute to Ca<sup>2+</sup> Gating

This reexamined Ano1 geography recommends additional opportunities for the instrument of channel gating by Ca<sup>2+</sup>. Amino acids 650 to 706, which were recently thought to shape an extracellular circle, contain an arrangement that is exceptionally preserved among all individuals from the Ano superfamily: [E/D]-[Y/F]-[M/L/Q]-E-[M/T/L/Q]. In Ano1 and Ano2, this arrangement is constantly 702EYMEM. To test whether this district is engaged with channel capacity, E702 and E705 in mAno1 were supplanted with glutamines. This twofold change displayed an obvious decrease in Ca<sup>2+</sup> affectability (Figure 2). The E702Q/E705Q freak was actuated just a limited quantity by 20  $\mu\text{mol/L}$  Ca<sup>2+</sup>, a fixation that maximally initiated wild-type (WT) Ano1, yet E702Q/E705Q was fundamentally enacted by 100-fold higher Ca<sup>2+</sup> focuses (2 mmol/L Ca<sup>2+</sup>). This grouping of Ca<sup>2+</sup> had no impact on Cl<sup>-</sup> flows in untransfected HEK cells (Online Figure I).

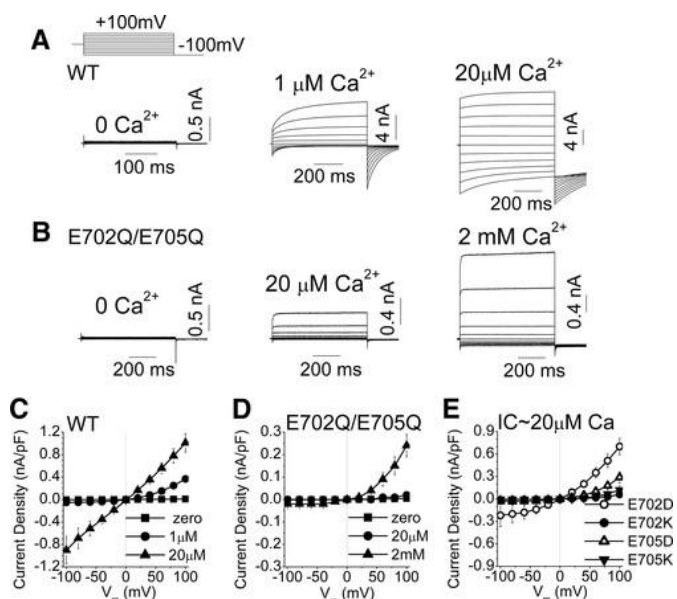


**Figure 2. Mutation of two critical amino acids, E702 and E705, dramatically affects Ca<sup>2+</sup>-gated but not voltage-gated current of mAno1.**

Representative whole-cell recordings of anoctamin-1 (Ano1) current in transfected HEK293 cells at the indicated free [Ca<sup>2+</sup>]. Voltage protocol is shown above (A). **A**, WT-mAno1. **B**, E702Q/E705Q mutant mANO1. Steady-state current–voltage (I–V) relationships for (C) WT-mAno1 and (D) E702Q/E705Q mANO1 with different [Ca]<sub>i</sub> (N=5–9). **E**, I–V relationships for E702D, E702K, E705D, and E705K mutants with 20 μmol/L Ca<sup>2+</sup> (N=5–9).

We have previously shown that Ano1 can be activated by high voltage in the absence of Ca<sup>2+</sup>. High-voltage-activated currents for E702Q/E705Q and WT were similar in amplitude (WT: 46.1±10.4 pA/pF, n=10; E702Q/E705Q: 45.0±7.6 pA/pF, n=5 at +200 mV; P=0.66), supporting the suggestion that this mutation mainly affects Ca<sup>2+</sup>-dependent gating while having little effect on voltage-dependent gating. Furthermore, the current activated by 500 μmol/L Ca<sup>2+</sup> was very strongly outwardly rectifying, which is characteristic of WT Ano1 currents that are activated by submaximal [Ca<sup>2+</sup>]. Voltage-dependent activation and deactivation of the current were accelerated as expected if the apparent affinity of the channel for Ca<sup>2+</sup> were decreased.

We then examined the effects of mutation of E702 and E705 individually. The conservative E702D substitution produced currents that were similar to WT but with slightly more outward rectification. In contrast, the charge-reversal E702K dramatically decreased Ca<sup>2+</sup>-activated current (Figure 2E). Both the conservative E705D and the charge-reversal E705K mutations exhibited markedly reduced Ca<sup>2+</sup>-dependent activation (Figure 2E). These results suggest that both E702 and E705 are important in Ca<sup>2+</sup> sensing or gating.

To quantify the effects of E702 and E705 substitutions on Ca<sup>2+</sup>-dependent gating, we performed experiments in which inside-out excised patches were rapidly

switched between zero and high Ca<sup>2+</sup> within several milliseconds (Figure 3). Current decay was well-fit by a monoexponential equation. The time constant of deactivation (τ<sub>off</sub>) was V<sub>m</sub>-dependent and was greatly accelerated by the E702Q and E705Q mutations (Figure 3E). At +120 mV, τ<sub>off</sub> was 408.4±67.3 ms for WT, 40.4±4.1 ms for E702Q, and 96.3±6.6 ms for E705Q.

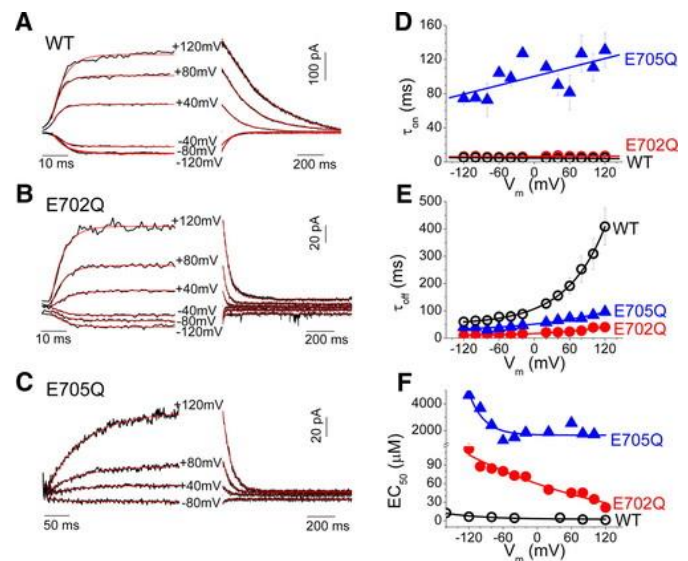


**Figure 3. Activation and deactivation kinetics of anoctamin-1 (Ano1) with rapid Ca<sup>2+</sup> perfusion in inside-out excised patches.** Representative traces of Ano1 current in response to application (left) and washout (right) of Ca<sup>2+</sup> at the indicated holding potentials. **A**, WT-mAno1. **B**, E702Q mANO1. **C**, E705Q mANO1. **D–F**, V<sub>m</sub> dependence of τ<sub>on</sub>, τ<sub>off</sub>, and EC<sub>50</sub> for WT Ano1 (open circles), E702Q (filled circles), and E705Q (filled triangles).

We have recently shown that Ano1 can be enacted by high voltage without Ca<sup>2+</sup>. High-voltage-initiated flows for E702Q/E705Q and WT were comparable in adequacy (WT: 46.1±10.4 pA/pF, n=10; E702Q/E705Q: 45.0±7.6 pA/pF, n=5 at +200 mV; P=0.66), supporting the idea that this transformation for the most part influences Ca<sup>2+</sup>-subordinate gating while at the same time having little impact on voltage-subordinate gating. Moreover, the current actuated by 500 μmol/L Ca<sup>2+</sup> was firmly obviously correcting, which is normal for WT Ano1 flows that are initiated

by submaximal  $[Ca^{2+}]$ . Voltage-subordinate actuation and deactivation of the current were sped up true to form if the obvious liking of the channel for  $Ca^{2+}$  were decreased.

We then, at that point analyzed the impacts of change of E702 and E705 separately. The traditionalist E702D replacement delivered flows that were like WT however with somewhat more outward amendment. Interestingly, the charge-inversion E702K drastically diminished  $Ca^{2+}$ -initiated current (Figure 2E). Both the traditionalist E705D and the charge-inversion E705K changes showed notably diminished  $Ca^{2+}$ -subordinate enactment (Figure 2E). These outcomes propose that both E702 and E705 are significant in  $Ca^{2+}$  detecting or gating.

To measure the impacts of E702 and E705 replacements on  $Ca^{2+}$ -subordinate gating, we performed tests in which back to front extracted patches were quickly exchanged among nothing and high  $Ca^{2+}$  inside a few milliseconds 18 (Figure 3). Current rot was very much fit by a monoexponential condition. The time steady of deactivation ( $\tau_{off}$ ) was  $V_m$ -subordinate and was enormously sped up by the E702Q and E705Q changes (Figure 3E). At +120 mV,  $\tau_{off}$  was  $408.4 \pm 67.3$  ms for WT,  $40.4 \pm 4.1$  ms for E702Q, and  $96.3 \pm 6.6$  ms for E705Q.

### Thiol Reagents Alter $Ca^{2+}$ Sensitivity of E702C and E705C

Alteration of the  $Ca^{2+}$  sensitivity of mAno1 by changing the charge at E702 and E705 by mutagenesis is consistent with the hypothesis that these amino acids contribute to a  $Ca^{2+}$  binding site. To test this hypothesis using a different approach, we asked whether modification of thiols introduced at these positions by charged MTS reagents would also alter  $Ca^{2+}$  sensitivity. The E702 or E705 were replaced with cysteine and the effects of charged thiol reagents, MTSET<sup>+</sup> and MTSES<sup>-</sup>, on channel gating by  $Ca^{2+}$  were measured in fast perfusion experiments. The MTS reagents were applied to the cytoplasmic face of inside-

out excised patches. The mAno1 has at least five cysteines that are predicted to be cytoplasmic, but neither MTSET<sup>+</sup> nor MTSES<sup>-</sup> had any significant effect on the amplitude or kinetics of activation or deactivation of WT mAno1 when applied to the cytoplasmic face of the patch (Figure 4C–E). The E702C (unmodified by MTS reagent) was much less sensitive to  $Ca^{2+}$  than WT mAno1. At +120 mV, the EC<sub>50</sub> for E702C was 114  $\mu$ mol/L compared to 0.94  $\mu$ mol/L for WT and 21  $\mu$ mol/L for E702Q. The larger EC<sub>50</sub> for E702C compared to E702Q might be explained if the side chain oxygen of glutamine participates in  $Ca^{2+}$  coordination. MTSET<sup>+</sup> increased the EC<sub>50</sub> of E702C approximately 30-fold (from 114  $\mu$ mol/L to approximately 3 mmol/L at 120 mV) by slowing  $\tau_{on}$  and accelerating  $\tau_{off}$  (Figure 4F–H). The decrease in  $Ca^{2+}$  affinity was accompanied by a decrease in current amplitude ( $56.4 \pm 10.8\%$ ), as expected. MTSES<sup>-</sup> had the opposite effect on EC<sub>50</sub> (Figure 4F–H) and the uncharged MTSEH had no effect (Online Figure IIIA). At 0 mV, the EC<sub>50</sub> was estimated to be 550  $\mu$ mol/L for unmodified E702C, approximately 3890  $\mu$ mol/L (extrapolated) for MTSET<sup>+</sup>-modified currents, and 144  $\mu$ mol/L for MTSES<sup>-</sup>-modified currents. The results with E705C exhibited a similar trend but were decidedly less dramatic, possibly because of reduced accessibility of MTS reagents to this residue, which is surrounded by very hydrophobic amino acids.

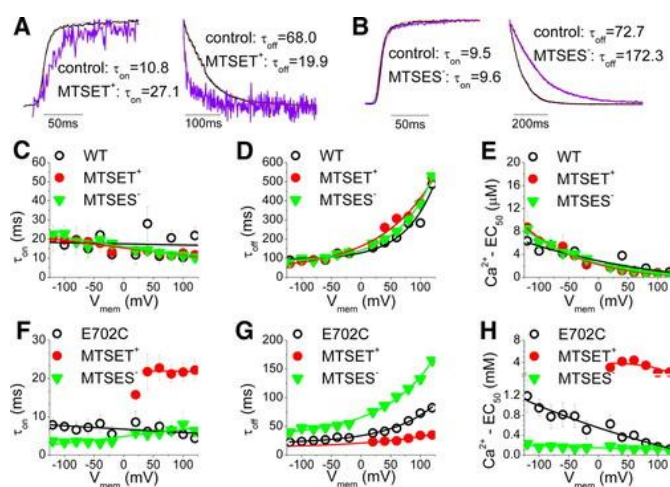


**Figure 4. Effects of sulfhydryl modification on activation and deactivation kinetics of anoctamin-1 (Ano1) in excised inside-out patches with rapid Ca<sup>2+</sup> perfusion.** Excised patches were switched between zero and high Ca<sup>2+</sup>. They were then exposed to MTS reagent in the presence of zero Ca<sup>2+</sup> for 10 seconds, MTS reagent was washed away, and the patch was switched from zero Ca<sup>2+</sup> to high Ca<sup>2+</sup> again. Normalized current traces of E702C mAno1 showing examples of changes in  $\tau_{on}$  and  $\tau_{off}$  caused by MTSET<sup>+</sup> (A) and MTSES<sup>-</sup> (B). Traces were normalized to the same maximal amplitude. As shown in Online Figure III, MTSET<sup>+</sup> causes a decrease in current and MTSES<sup>-</sup> increases the current. The magnitude of the effect of MTS reagent on current amplitude depends on where on the Ca<sup>2+</sup>dose–response curve the experiment is performed. C–E, Lack of effect of MTS reagents on  $\tau_{on}$ ,  $\tau_{off}$ , and EC<sub>50</sub> for WT Ano1. F–H, Effects of MTS reagents on  $\tau_{on}$ ,  $\tau_{off}$ , and EC<sub>50</sub> for E702C mAno1. Open circle: before application of MTS reagent. Filled circle: after MTSET<sup>+</sup>. Triangle: after MTSES<sup>-</sup>. N=3–6.

If E702 and E705 are located on the cytoplasmic side of the membrane, we would predict that MTS reagents applied from the extracellular side would have no effect on E702C or E705C currents. We tested this prediction using whole-cell recording because outside-out patches could be obtained with only very low success. We also tested several other cysteine-substituted amino acids nearby. In whole-cell recording, extracellular application of MTSET<sup>+</sup> and MTSES<sup>-</sup> had no significant effect on E702C or E705C currents (MTSET<sup>+</sup> increased E702C currents by 4.7%±6.6% and decreased E705C by -3.1%±0.9%). This compares to a decrease of 56.4%±10.8% for E702C in excised patches exposed to cytosolic MTSET<sup>+</sup>. MTSET<sup>+</sup> had no significant effect on any of the currents generated by these cysteine-substituted mutants (Online Figure IIIB).

Online Figure IV shows the time courses of the current changes caused by cytoplasmic MTS reagents on

E702C and WT in inside-out excised patches. Currents were activated by a low concentration of Ca<sup>2+</sup> to maximize the change in current amplitude that was produced by a change in Ca<sup>2+</sup> affinity. MTSET<sup>+</sup> (1 mmol/L) decreased the current with  $\tau$  of 52 ms and a rate constant of approximately  $2 \times 10^4 \text{ M}^{-1}\text{s}^{-1}$ . This rate is close to the rate of modification of mercaptoethanol by MTSET<sup>+</sup> in solution (approximately  $10^5 \text{ M}^{-1}\text{s}^{-1}$ ), suggesting that these residues are freely accessible to the aqueous environment. The effect of MTSES<sup>-</sup> is slower than MTSET<sup>+</sup>, but because MTSES<sup>-</sup> reacts with mercaptoethanol in solution approximately five-times slower than MTSET<sup>+</sup>, this result is also consistent with high aqueous accessibility.

### Sources of Funding

Supported by grants from the National Institutes of Health GM60448 (H.C.H.), EY014852 (H.C.H.), the Microscopy Core of the Emory Neuroscience NINDS Core Facilities grant P30NS055077, and NEI Core grant P30EY006360. C.D. was supported by NEI training grant 5T32EY007092-25.

### Disclosures

None.

This work is partly presented at 24th World Chemistry & Systems Biology Conference on October 03-04, 2018 in Los Angeles, USA